



Received: 11/03/2024

Accepted: 28/03/2024

Anales de Edificación
Vol. 10, Nº1, 33-44 (2025)
ISSN: 2444-1309
DOI: 10.20868/ade.2025.5386

FRCM Composites para aplicaciones estructurales: una revisión sistemática

FRCM Composites for structural applications: a systematic review

María Rodríguez Marcos^a; Paula Villanueva Llauradó^b; Jaime Fernández Gómez^a

^a Departamento de Ingeniería Civil: Construcción, ETSICCP, Universidad Politécnica de Madrid (UPM), Spain;
m.rmarcos@alumnos.upm.es jaime.fernandez.gomez@upm.es

^b Departamento de Estructuras y Física de edificación, ETSAM, Universidad Politécnica de Madrid (UPM), Spain;
paula.villanueva@upm.es

Resumen-- Las matrices cementosas reforzadas con fibras (MCRF) son materiales compuestos que se utilizan cada vez más para la rehabilitación de estructuras existentes debido a su elevada relación resistencia-peso. Las FRCM están formadas por un tejido embebido en una matriz de mortero. Generalmente, el textil es una rejilla ortogonal que puede estar hecha de fibras de carbono, vidrio resistente a los álcalis (AR), basalto, aramida o PBO. Los morteros pueden ser a base de cal o cementosos, y pueden incluir varias adiciones como polímeros, fibras y cenizas volantes.

En este trabajo, para investigar sistemáticamente el comportamiento mecánico de los materiales compuestos FRCM sometidos a esfuerzos de tracción, así como el comportamiento en la interfaz FRCM-hormigón sometida a flexión, se realizó una revisión exhaustiva de los estudios experimentales.

Se diseñó un protocolo para la revisión sistemática, en el que la selección de artículos estuvo motivada por la inclusión de investigaciones experimentales, dentro del corpus de Web of Science de artículos que trataban sobre materiales FRCM de carbono, mediante la inclusión de «carbono» en el resumen o en el título.

Palabras clave— Matriz cementosa reforzada con fibras; Resistencia a la tracción; Resistencia a la flexión; Sistema de retroadaptación.

Abstract— Fibre Reinforced Cementitious Matrices (FRCM) are composite materials which are being increasingly used for retrofitting of existing structures due to their high strength-to-weight ratio. FRCM consists of a textile embedded in a mortar matrix. Generally, the textile is an orthogonal grid which can be made of carbon fibres, alkaline resistant (AR) glass, basalt, aramid, or PBO. Mortars can either be lime-based or cementitious, and may include several additions such as polymers, fibres and fly ash.

In this work, to systemically investigate the mechanical performance of FRCM composites subjected to tensile stresses as well as the behaviour in the FRCM-to-concrete interface subjected to flexure, a comprehensive review was conducted on experimental studies.

A protocol was designed for the systematic review, in which selection of papers was motivated by the inclusion of experimental research, within the Web of Science corpus of papers dealing with Carbon FRCM materials, by inclusion of “carbon” either in the abstract or in the title.

Index Terms— Fibre Reinforced Cementitious Matrix; Tensile strength; Flexural strength; Retrofitting system.

I. INTRODUCTION

Fibre Reinforced Cementitious Matrix (FRCM) are composite materials used for structural retrofitting due to their high strength-to-weight ratio (Arboleda *et al.*, 2016;

Carozzi & Poggi, 2015; Tommaso D’Antino *et al.*, 2014). They are formed by a textile embedded in a mortar matrix. Generally, the textile is an orthogonal grid of fibres made of carbon, alkaline resistant (AR) glass, basalt, aramid or synthetic polymer reinforcements such as PBO. The carbon fibres have

M.R.M. is PhD student at Civil Engineering Department, construction section from Universidad Politécnica de Madrid. J.F.G. is associate professor at Civil Engineering Department, construction section from Universidad Politécnica de Madrid. P.V.L.L. is associate professor at Structures and Building

Physics at Escuela Técnica Superior de Arquitectura de Madrid from Universidad Politécnica de Madrid.

higher strength and stiffness and, also, they are lighter, though the material is more expensive, it is fragile. This type of fibres, together with AR glass fibres, are the most used. Mortars can be lime-based or cementitious, and can include several additions such as polymers, fibres and fly ash (Bertolesi *et al.*, 2014; Bilotta *et al.*, 2017; Caggegi, Carozzi, *et al.*, 2017; Caggegi, Lanoye, *et al.*, 2017; Carozzi *et al.*, 2017b; de Felice *et al.*, 2020; Donnini *et al.*, 2019; Leone *et al.*, 2017; Lignola *et al.*, 2017; Mazzucco *et al.*, 2018; Ombres *et al.*, 2019; Catherine G. Papanicolaou *et al.*, 2008; Tekieli *et al.*, 2017).

The main advantages of FRCM systems compared with the more widespread use of FRP are: higher temperature resistance and even fire resistance thanks to cementitious matrix which performs similarly to concrete and masonry structures in case of fire, ability to be applied in wet surfaces, higher compatibility with masonry structures and vapour permeability (Arboleda *et al.*, 2016; Awani *et al.*, 2015; Bertolesi *et al.*, 2014; Butler *et al.*, 2010; Tommaso D'Antino & Papanicolaou, 2018; de Felice *et al.*, 2014; De Santis & De Felice, 2015; Donnini *et al.*, 2016; Escrig *et al.*, 2015; Ombres, 2015; C G Papanicolaou & Papantoniou, 2016; Catherine G. Papanicolaou *et al.*, 2008; Peled *et al.*, 2017; Tetta & Bourmas, 2016; Valluzzi *et al.*, 2014). On the other hand, FRP systems typically present reinforcement-to-substrate failure, with the reinforcement keeping the composite performance, while the FRCM may present a premature slippage of the fibres within the matrix, thus losing the composite behaviour and limiting the overall performance of the reinforcement.

Before designing a FRCM structural reinforcement, it is necessary to assess the mechanical properties of the system through tensile and flexural tests. The mechanical properties can largely differ among FRCM systems, depending both on textile and matrix characteristics and on their interfacial performance, as well as the support characteristics. As previously mentioned, the bond between the two components has a high influence in the overall behaviour of the composite, controlling the load transfer mechanism and being responsible of premature failure. The matrix may be unable to fully penetrate inside the yarn, so dry fibres rovings are generally not impregnated and the behaviour of the outer filament differs from that of the inner ones (T. D'Antino & Papanicolaou, 2017; Peled *et al.*, 2008; Peled & Bentur, 2000). Therefore, the inner filaments can have a slippage (telescopic behaviour) which can be prevented by employing coatings or impregnation systems able to penetrate inside the yarn. Also, such coating may serve to protect the fibres and to improve the adhesion to the matrix (T. D'Antino & Papanicolaou, 2017; Hartig *et al.*, 2012).

Typically, FRCM systems show an idealized trilinear stress-strain curve under uniaxial tensile stress as in Fig. 1. Each branch corresponds to a different cracking state. At the beginning there is an elastic phase (stage A), in which the applied load is carried by the uncracked matrix and the stiffness of the system is supposed to be like that of the mortar. When the tensile strength of the mortar is reached, the first crack appears, and the second phase starts (stage B). The slope of the stress-strain curve decreases during this phase, and the load is

mainly transferred from the matrix to the embedded fibres. In the last phase (stage C), when the matrix is fully cracked, the existing cracks only increase their width; at this stage the textile is the responsible for sustaining the whole load, so stiffness and tensile strength can be related to textile properties. This third phase can either be present or not depending on the slippage between fibres and matrix, especially in composites with low strength matrix. In this paper, the existence or not and the effects on ultimate load of the trilinear behaviour were some of the analysed parameters.

In this work, to systemically investigate the mechanical performance of FRCM composites subjected to tensile stresses as well as the behaviour in the FRCM-to-concrete interface subjected to flexure, a comprehensive review was conducted on experimental studies from 2015 to 2022 for tensile tests and from 2011 to 2022 for flexural tests. Following this search, the beams with FRCM shear reinforcement were excluded from the analysis.

A protocol was designed for the systematic review, in which selection of papers was motivated by the inclusion of experimental research, within the Web of Science corpus of papers dealing with Carbon FRCM materials, by inclusion of "carbon" either in the abstract or in the title. This means that the research was restricted to CFRM, being carbon the most widely used fibre type for concrete retrofitting.

The parameters that were chosen for assessment of tensile tests were:

- Matrix properties: compressive strength, tensile strength and E.
- Textile properties: grid spacing, coating (if any), density, tensile strength, E, ultimate strength.
- Specimen characteristics: length, width, thickness, number of tensile longitudinal threads, textile cross section or volumetric percentage of reinforcement
- Monitoring and testing: type of monitorization and data acquisition, test type and test parameters (test speed)
- Results: identification of modulus of elasticity and tensile strength for each branch, number of identifiable branches in the stress-strain behaviour under tensile stresses.

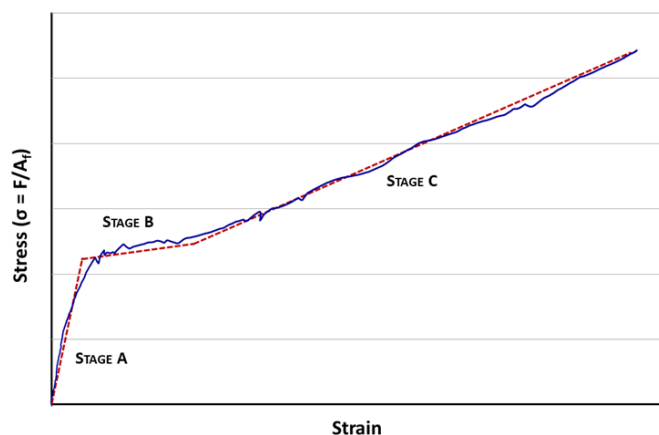


Fig. 1. Typical stress-strain curve for FRCM systems modified from CNR-DT 215 (2018) (Guide for the Design and Construction of Externally Bonded FRP Systems for Strengthening Existing Structures, 2018).

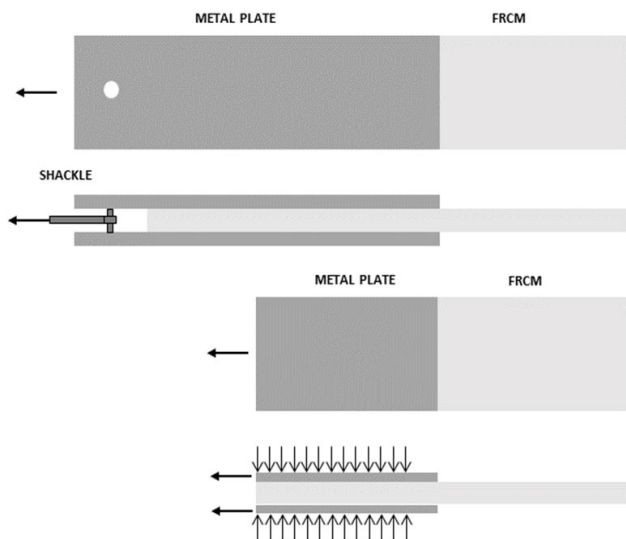


Fig. 2. Support systems: a) clevis b) clamping

Similarly, for flexural tests the following parameters were studied:

- Support properties (size, material, in case of concrete compressive and tensile strength) and existence and (in any), arrangement of internal reinforcement.

- Reinforcement properties: textile and matrix properties, composite behaviour, arrangement of main reinforcement and existence of shear/anchorage systems
- Monitorization and testing: type of monitorization and data acquisition, test type (intermediate supports, number of loading points) and test parameters (test speed)
- Results: crack load and ultimate load, ratio of improvement with FRCM reinforcement versus control tests, failure mode.

II. DATABASE

A database was created based on the bespoke parameters for tensile and flexural tests. Apart from differences in the material properties of support and reinforcement, the influence of the test arrangement was considered in the study as there is an important variation within the literature. In Fig. 2, the differences between the two more widely used support systems for tensile tests are graphically presented.

Table 1 presents the collected database for tensile tests, comprising the data acquisition and support systems, as well as the test speed and the parameter of coated versus dry grids.

TABLE I
 DATABASE FOR TENSILE TEST

Authors	Year	Type of samples	Coating	Speed [mm/min]	Data acquisition	Support System
Arboleda, 2014	2014	1	-	0.25	-	-
Arboleda <i>et al.</i> , 2016	2015	4	Dry (2) Coated (2)	0.25	Extensometer LVDT;	Clevis (3) Clamping (1)
Ascione <i>et al.</i> , 2015	2015	1	Dry	0.6	Extensometer; Potenciometer	Clamping
Bellini <i>et al.</i> , 2019	2019	2	Dry	0.1-0.2	Extensometer LVDT; DIC;	Clamping
Carozzi <i>et al.</i> , 2017a	2017	13	Dry (3) Coated (6)	0.1-1	Extensometer; Potenciometer	Clevis (1) Clamping (11)
Carozzi & Poggi, 2015	2015	1	Dry	0.1-0.5	Extensometer LVDT;	Clamping
Choi <i>et al.</i> , 2021	2021	2	-	1	Extensometer	Clevis
Tommaso D'Antino & Papanicolaou, 2017	2017	4	Dry (1) Coated (3)	0.5	2 LVDT	Clamping
Tommaso D'Antino & Papanicolaou, 2018	2018	4	Dry (2) Coated (2)	0.5	LVDT, DIC, Gauge length	Clamping
De Domenico <i>et al.</i> , 2022	2022	3	Dry (3)	0.2	Extensometer	Clevis
de Felice <i>et al.</i> , 2020	2020	2	Coated	-	-	-
De Santis <i>et al.</i> , 2018	2018	2	-	0.25-0.3	Extensometer	Clevis (1) Clamping (1)
Donnini <i>et al.</i> , 2016	2016	14	Dry (3) Coated (11)	0.3	Extensometer	Clevis
Ebead <i>et al.</i> , 2017	2017	1	-	0.25	Displacement transducer	Clevis
Estevan <i>et al.</i> , 2022	2022	1	Coated	0.2	LVDT; DIC	-
H.-S. Kim <i>et al.</i> , 2018	2018	6	-	0.5	LVDT	Clamping
Rodríguez-Marcos <i>et al.</i> , 2023	2023	8	Dry (3) Coated (5)	0.5	DIC	Clamping
Mei ni Su <i>et al.</i> , 2022	2022	8	Dry (6) Coated (2)	0.2	2 LVDT	Clevis
Tran <i>et al.</i> , 2019	2019	9	Dry (3) Coated (6)	0.5	2 LVDT	Clamping
Truong <i>et al.</i> , 2021	2021	9	Dry (7) Coated (2)	1	2 LVDT, DIC	Clamping
L. L. Wei <i>et al.</i> , 2020	2020	7	-	0.2	Extensometer	Clevis
Younis <i>et al.</i> , 2020	2020	4	Dry	0.25	Extensometer	Clevis

TABLE II
DATABASE FOR FLEXURAL TEST

Authors	Year	Type of samples	Coating	Speed [mm/min]	Data acquisition	Support System
(Akbari Hadad <i>et al.</i> , 2018)	2018	3	Bottom	1/2	Strain gauges, LVDT	3 points
(De Santis <i>et al.</i> , 2018)	2020	4	Bottom	1/4	Strain gauges, 2 LVDT	4 points
(Bressan <i>et al.</i> , 2022)	2022	2	Bottom with anchor	2	Strain gauges, 2 LVDT	4 points
(D’Ambrisi <i>et al.</i> , 2013)	2013	6	Bottom/ with anchor/ with U	2	Strain gauges	4 points
(Ebead & El-Sherif, 2019)	2019	4	Bottom	1	Strain gauges, 2 LVDT	4 points
(Ebead <i>et al.</i> , 2017)	2017	6	Bottom	1/2/3	Strain gauges, LVDT	4 points
(El-Sherif <i>et al.</i> , 2020)	2020	2	Bottom	4	Strain gauges, LVDT	4 points
(Elghazy <i>et al.</i> , 2017)	2017	3	Bottom with U	3	Strain gauges	4 points
(Elghazy <i>et al.</i> , 2018)	2018	2	Bottom with U	2/3	Strain gauges	4 points
(Feng <i>et al.</i> , 2020)	2020	8	Bottom and top/ with U	2/3	Strain gauges, 5 LVDT	5 points
(Jabr <i>et al.</i> , 2017)	2017	2	Bottom with U	2	Strain gauges, 3 LVDT	4 points
(Khattak <i>et al.</i> , 2021)	2021	4	Bottom	2/4	Strain gauge, 2 LVDT	5 points
(H.-Y. Kim <i>et al.</i> , 2022)	2022	5	Bottom/with anchor	1	2 LVDT	3 points
(H.-Y. Kim <i>et al.</i> , 2021)	2021	4	Bottom	1	2 LVDT	3 points
(H.-Y. Kim <i>et al.</i> , 2020)	2020	6	Bottom	1/2	Strain gauges, LVDT	4 points
(Mandor & El Refai, 2022)	2022	2	Top with U/ Bottom with U	2	Strain gauges, 6 LVDT	5 points
(Raof & Bournas, 2017)	2017	4	Bottom/ with anchor	1/3	2 LVDT	4 points
(Raof <i>et al.</i> , 2017)	2017	5	Bottom with U	1/3/5	2 LVDT	4 points
(Mei-ni Su, Wei, Zhu, <i>et al.</i> , 2019)	2021	2	Bottom	2	Strain gauges	4 points
(Mei-ni Su <i>et al.</i> , 2020)	2020	5	Top and bottom/ top/ bottom	2	Strain gauges, 4 LVDT	5 points
(Mei-ni Su, Wei, Zeng, <i>et al.</i> , 2019)	2019	4	Bottom	1	3 LVDT	4 points
(L. Wei <i>et al.</i> , 2021)	2021	3	Bottom	1/2/4	Strain gauge, extensometer, 3 LVDT	4 points

On the other hand, in flexural tests it was found that the variability was much greater. The main arrangements depended on whether the reinforcement was designed for either negative or positive bending moment. Also, in some cases, different anchorage systems were used to prevent debonding, in similar arrangements to those of FRP reinforcements. In Fig. 3, test arrangements for flexural test in the database are summarised.

As previously mentioned, the different arrangements are related to the number of supports and, consequently, to the number of points in the test. Table 2 presents the collected database for flexural tests, summarising the test arrangement, the number of layers of reinforcement in the different tests, and the data acquisition system.

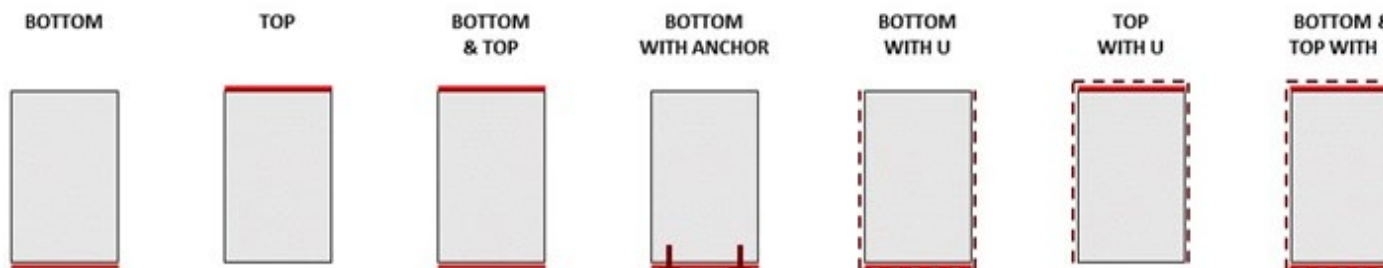


Fig. 2. Support systems: a) clevis b) clamping

III. DISCUSSION

A. Tensile test.

The differences in terms of the exploitation ratio (ultimate tensile strength of the composite to tensile strength of the textile), regarding the test system, were statistically analysed. The distribution is not normal, and it was found that no significant statistical difference exists between clamping and clevis system. Fig. 4. shows the exploitation ratio for clamping and clevis systems. Mean exploitation ratio and standard deviation for clamping system is $63.03\% \pm 81.70\%$ and for clevis is $60.92\% \pm 48.21\%$. Nevertheless, it was observed that trilinear behaviour in the stress-strain curves only appeared when clamping systems were employed. Also, for specimens with the same mortar and grid, clamping system obtained better results in terms of ultimate load, as can be observed in the results by D. A. Arboleda, F.G. Carozzi and A. Nanni (2016)(Arboleda *et al.*, 2016). The ultimate tensile strength for camping system was 1492 MPa while for clevis was 1031 MPa.

Similarly, an analysis was performed to compare coated and non-coated fibres. The distribution in not normal and there are no statistical differences between groups. The mean and standard deviation were $84.72\% \pm 94.62\%$ for coated grids and $47.44\% \pm 30.05\%$ for dry ones. Fig. 5 corresponds to the exploitation ratios for each group. Generally, it is more common to obtain trilinear stress-strain curves for coated textiles (Carozzi *et al.*, 2017b; Tommaso D’Antino & Papanicolaou, 2017, 2018; Rodríguez-Marcos *et al.*, 2023; Truong *et al.*, 2021) than for dry grids (Arboleda *et al.*, 2016; Bellini *et al.*, 2019; Carozzi *et al.*, 2017b; Carozzi & Poggi, 2015).

Fig. 6 collects the idealized stress-strain curves for the analysed tests. The tests were grouped according to the test configuration and coated versus uncoated grids. Blue lines correspond to dry textile, red lines to coated textile and grey lines to non-specified. The dashed lines are for clevis systems and the continuous for clamping. The higher precracking strength and ultimate strength of a group of samples with impregnated textile and tested with clamping can be clearly seen. Due to the large number of tests, the curves are grouped by coating and test type for easier analysis

Fig. 7 and 8 show the idealized stress-strain curves for, respectively, uncoated and coated FRCM systems. Each Fig. has two graphics depending on the test system. The scale for stress is limited to 2000 MPa in uncoated systems and 7000 MPa in coated systems, so the curves with different coating cannot be compared directly. The number of dry textile samples tested with clevis is 12 and with clamping is 24. There is a greater dispersion in clamping samples, although there is also greater variability in the properties of the meshes. The sample with a compressive strength of 48 MPa and a textile tensile strength of 4800 MPa tested with clamping is the unique FRCM system with pre-cracking strength higher to 1000 MPa (Rodríguez-Marcos *et al.*, 2023).

Coated textile grids are studied to a lesser extent than uncoated grids, the number of samples tested with impregnated grids is 26 versus 36 with dry fibres. Although in the case of coated meshes, the use of clamping systems is much greater (23 samples) than clevis system (3 samples). There are clearly two groups in the systems tested with clamping, the samples with

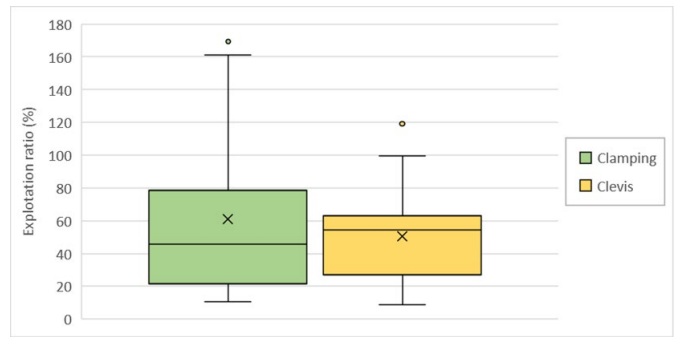


Fig. 4. Exploitation ratio depending on the support system.

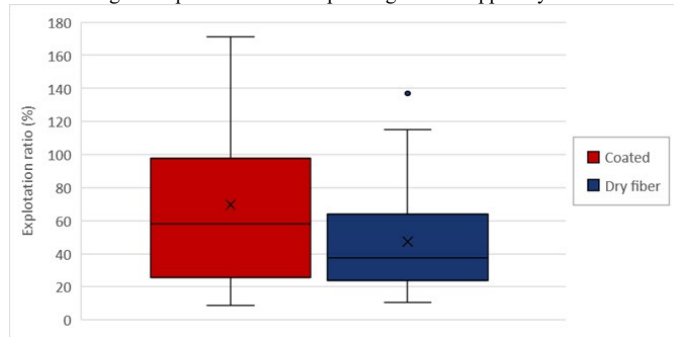


Fig. 5. Exploitation ratio depending on the coating of the textiles.

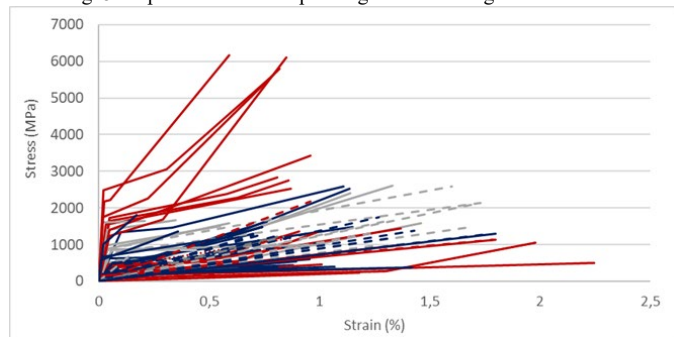


Fig. 6. Stress-strain idealized curves for FRCM systems. Blue lines are for dry textile, red for coated textile and grey lines for not specified. Dash lines are for clevis and continuous lines for clamping.

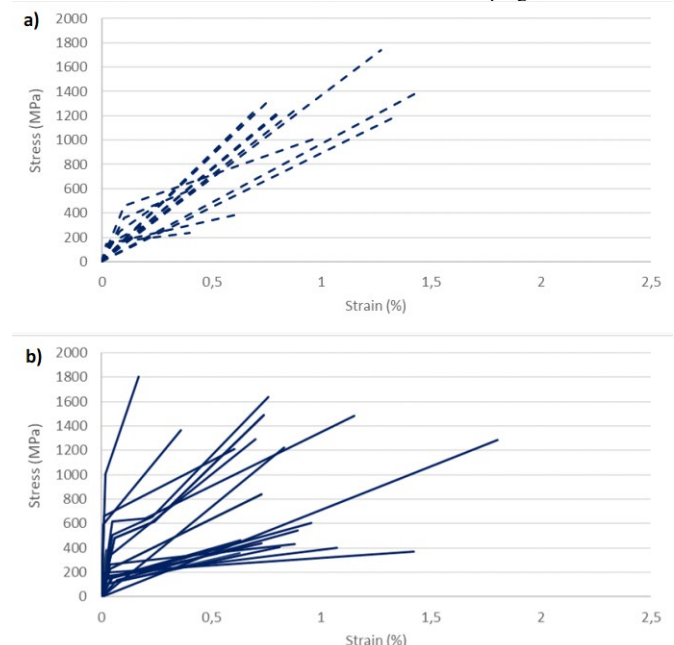


Fig. 7. Stress-strain idealized curves for FRCM systems for dry textile. a) Clevis b) Clamping.

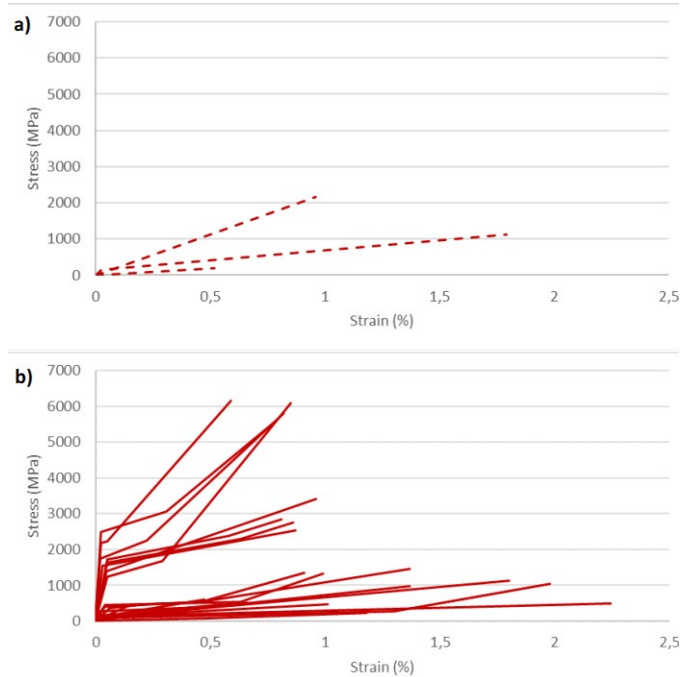


Fig. 8. Stress-strain idealized curves for FRCM systems for coated textile. a) Clevis b) Clamping

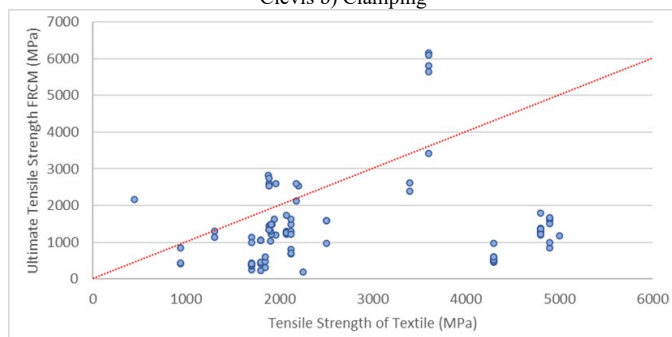


Fig. 9. Ultimate strength of FRCM versus tensile strength of textile

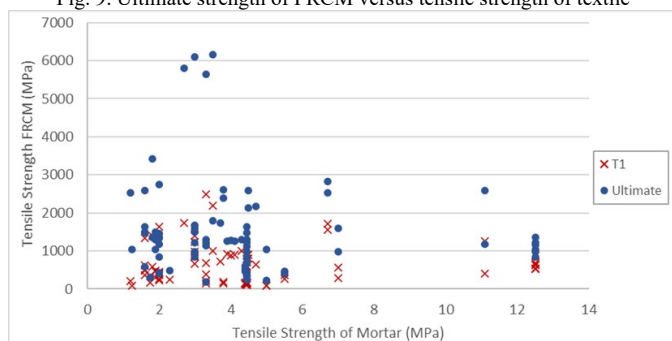


Fig. 10. Pre cracking and ultimate tensile strength of FRCM versus tensile strength of mortar

better behaviour have a pre-cracking strength higher than 1000 MPa and ultimate strength higher than 2500 MPa (Carozzi *et al.*, 2017b; Tommaso D’Antino & Papanicolaou, 2017; Rodríguez-Marcos *et al.*, 2023). The samples with worst behaviour have a pre-cracking strength lower than 500 MPa and an ultimate tensile strength lower than 1500 MPa, also, the ultimate strain for this group is bigger. It should be noted that the mechanical properties of the textile and matrix are similar in both groups, as well as test set up, the only possible difference being the type of coating (acrylic resin and epoxy resin).

Fig. 9 presents the results in terms of ultimate stress versus rupture stress of the grid. It can be observed from Fig. 10. that most textiles have a tensile strength within the range of 1500-2500 MPa. Within this group, there is a large variation in terms of ultimate strength of the composite material, ranging from 1000 to 3000 MPa with no correlation between the tensile strength of the textile and that of the FRCM. There is a small group of samples, corresponding to 3500-4000 MPa of the textile, in which the overall exploitation of the composite material is remarkable, achieving ultimate tensile strengths up to twice that of the textile. No significance improvement seems to be achieved increasing the tensile strength of the grid up to 5000 MPa, given that the performance depends more on matrix-to-grid adherence and slippage than on failure of the textile. The 12 samples (Bellini *et al.*, 2019; Carozzi *et al.*, 2017b; Choi *et al.*, 2021; Tommaso D’Antino & Papanicolaou, 2017; De Santis *et al.*, 2018; Rodríguez-Marcos *et al.*, 2023; Mei ni Su *et al.*, 2022) with higher ultimate tensile strength than ultimate textile strength have different mechanical properties of textile (tensile strength from 441 MPa to 3600 MPa) and matrix (mortar compressive strength from 10 MPa to 71 MPa), different test set up (clevis and clamping) and the textile is coated and uncoated. It can be concluded, then, that no individual parameter was determinant for such good performance, as they do not share any characteristic.

Fig. 11 presents the results in terms of ultimate stress versus pre-cracked stress and versus ultimate stress in the mortar. For each tensile strength of the mortar, there is a pair of FRCM values, the cross corresponds to the crack initiation (T1) and the dot to ultimate strength. There is no correlation between mortar strength and FRCM strength, neither cracking nor ultimate strength. The most common tensile strength for the mortar is between 2 and 6 MPa and the highest composite strength around 3 MPa. The cracking resistance of the FRCM does not affect the ultimate strength, the ratio between ultimate strength and cracking resistance is between 2 and 4 for the FRCM systems with the highest ultimate strength. The tensile strength of the mortar neither affects the relationship of ultimate and cracking strengths, as the highest ratios were found for strengths below 5 MPa.

B. Bending test.

The analysis was focused on flexural performance, thus assessing the relevance of the inclusion of anchorage systems for the longitudinal reinforcements, and the differences in terms of isostatic and hyperstatic beams.

The first analysis comprises the comparison in terms of failure modes. In Fig. 11, the distribution of failure modes for different beam configurations is presented.

It can be observed from Fig. 12. that the prevailing failure modes are slippage of the textile within the matrix and debonding at the matrix-to-textile interface. These, together with slippage of the textile and cracking of the outer layer of mortar, are similar failure modes, defined in CNR DT 215/2018 (Guide for the Design and Construction of Externally Bonded FRP Systems for Strengthening Existing Structures, 2018). In all cases, they correspond to insufficient adherent strength between the matrix and the textile, the main difference being the complete detachment of some layers of textile from the first

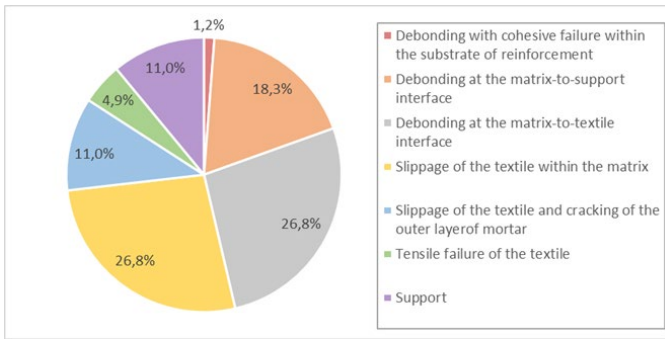


Fig. 11. Failure modes

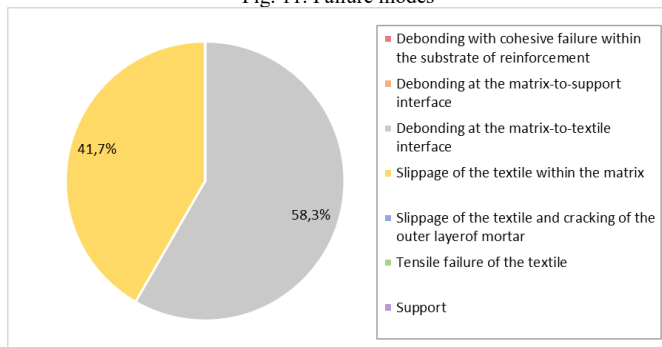


Fig. 2. Failure modes bending 3 points.

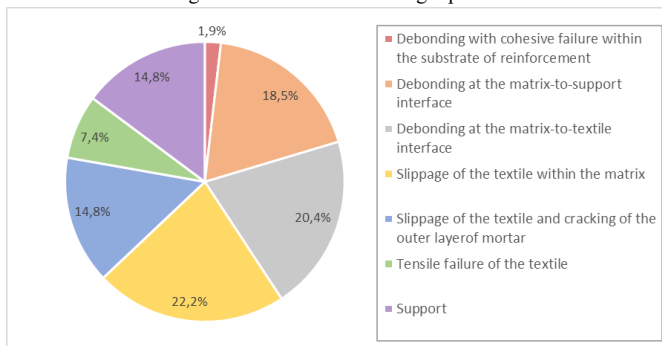


Fig. 3. Failure modes bending 4 points.

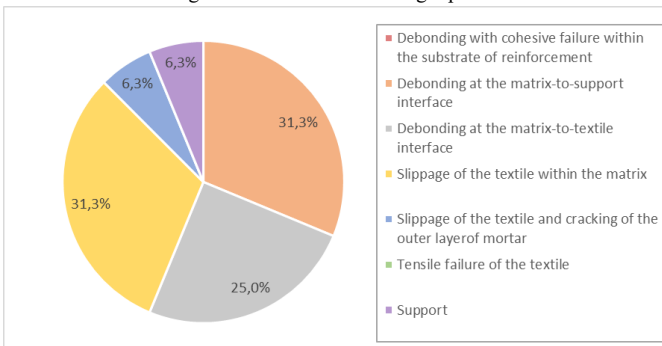


Fig. 4. Failure modes bending 5 points.

layer of matrix, or the preservation of some adherence between different layers of matrix. They correspond to undesired failure modes related to the poor adherence previously reported in most tensile tests, which hinders full exploitation of the composite properties.

The reason for support failure can be found in an optimised design of the test and specimen size according to the ratio of reinforcement (H.-Y. Kim *et al.*, 2020), and this was only achieved in 11% of all tests. Also, this failure mode can be due to insufficient section in the concrete corresponding to low ultimate loads independently from the reinforcement design,

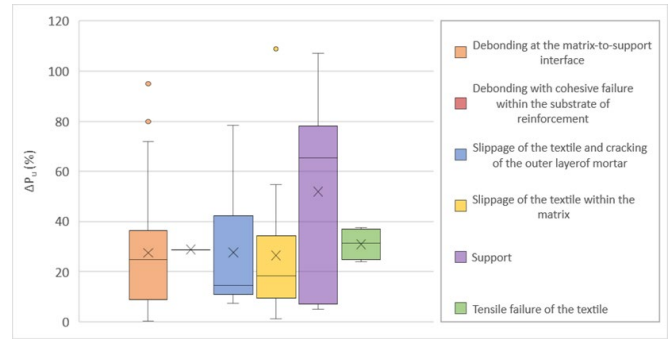


Fig. 15. Ratio ultimate load/control load (ΔP_u) depending on failure mode.

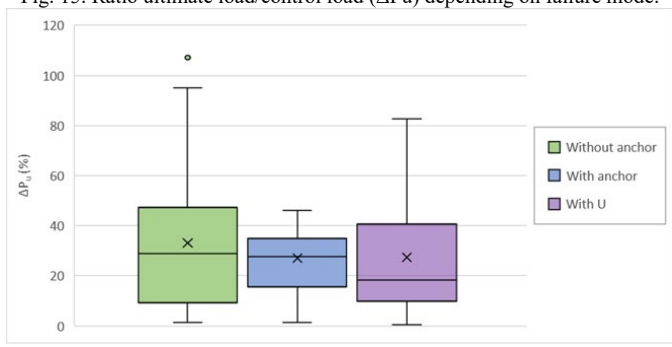


Fig. 16. Ratio ultimate load/control load (ΔP_u) depending on the existing and type of anchoring system.

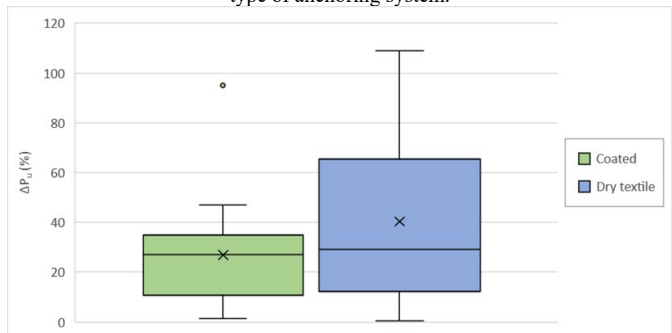


Fig. 17. Ratio ultimate load/control load (ΔP_u) depending on the coating of the textile.

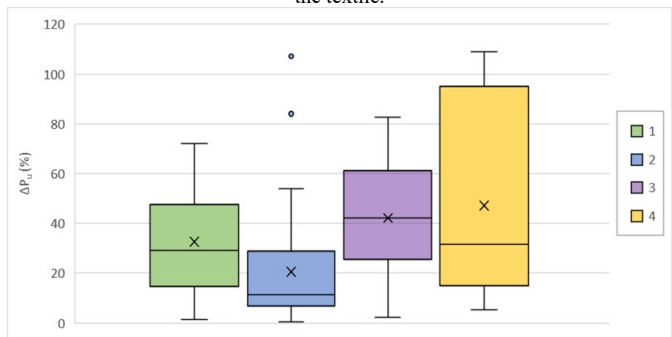


Fig. 18. Ratio ultimate load/control load (ΔP_u) depending on the number of layers of textile.

prior to other failures, or even to low exploitation of the reinforcement for high ultimate load of the control beams (Mandor & El Refai, 2022; Mei-ni Su *et al.*, 2020).

It is more interesting the 19,5% of tests that achieved debonding at the matrix to support interface and the support, this being a failure mode closely related to FRP composites, in which the composite material behaviour is maintained until failure of the structure. In this case, depending on adherent properties in the substrate to matrix interface, it is possible to observe a cohesive failure (Khattak *et al.*, 2021) or (more

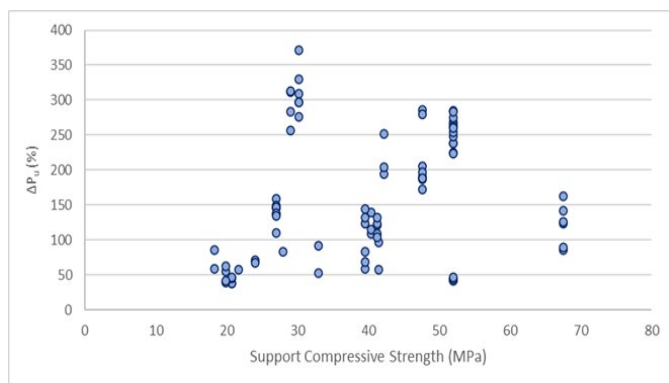


Fig. 19. Ratio ultimate load/control load (ΔP_u) versus support compressive strength

commonly) detachment of the reinforcement (Feng *et al.*, 2020; H.-Y. Kim *et al.*, 2022; Raof *et al.*, 2017; Raof & Bournas, 2017; L. Wei *et al.*, 2021).

Fig. 12, Fig. 13 and Fig. 14 correspond to failure modes depending on the type of test: 3 points, 4 pints and 5 points, respectively.

The mechanical and geometrical properties of the beams and their components, as well as the test set-up of the beams with a load increment in the upper 10% range, were analysed. The samples were taken from 6 papers (Akbari Hadad *et al.*, 2020; Ebead *et al.*, 2017; El-Sherif *et al.*, 2020; Elghazy *et al.*, 2018; H.-Y. Kim *et al.*, 2020; Raof *et al.*, 2017), and all were tested in 4-point bending. The reinforcement was on the bottom face and only one of the beams had a U-shaped anchorage (Elghazy *et al.*, 2018). The failure mode is not common: three of the beams failed at the support (H.-Y. Kim *et al.*, 2020), those corresponding to the slab-type beam with a depth of 20 cm, a width of 1 m and a length of 1.8 m; two failed by slippage of the textile (within matrix and cracking the outer layer of mortar) (Ebead *et al.*, 2017; El-Sherif *et al.*, 2020), one failed by debonding at matrix-to-support interface (Raof *et al.*, 2017) and one failed by debonding at the matrix-to-textile interface (Akbari Hadad *et al.*, 2020). The compressive strength of the beam concrete ranged from 20 MPa to 68 MPa, with compressive strength of 40 MPa for the beam with the largest increment (El-Sherif *et al.*, 2020). Most of the meshes were uncoated, the only beam reinforced with a coated textile had an increment in the ultimate load/control load of 95% (Akbari Hadad *et al.*, 2020). The tensile strength of the meshes was very variable (450-4800), as was the number of layers employed (1-5). The beam reinforced with the highest textile strength (4800 MPa) and five layers had the highest increment (El-Sherif *et al.*, 2020). The Fig. 15. corresponds to the ratio ultimate load/control load depending on the failure mode. All the samples exhibiting textile failure had an ultimate load increment between 20 MPa and 40 MPa, which is the smallest range of all failure modes. On the other hand, the failure due to support had the largest range, the lower ratio ultimate load/control load are the result of incorrect design of the support (high strength of the control specimens without need of reinforcement or too low ultimate loads independently from the reinforcement design) and higher increments were caused by fuller exploitation of the reinforcement.

Fig. 16 presents the differences in terms of the ratio ultimate load/control load for anchored and unanchored flexural

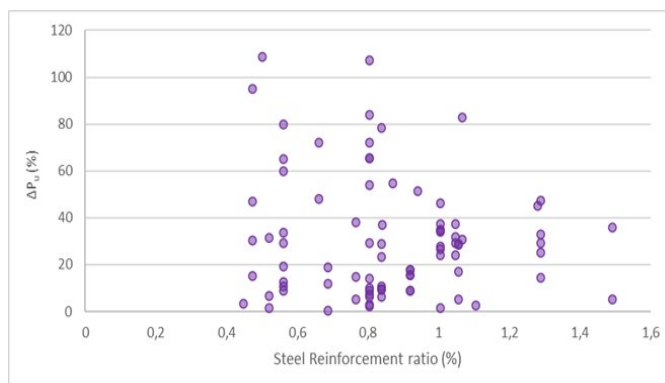


Fig. 20. Ratio ultimate load/control load (ΔP_u) versus steel reinforcement ratio.

reinforcements. The distribution is not normal, and it was found that no significant statistical difference exists between unanchored, anchored, nor within the anchored samples with different anchor types. Mean ultimate load increment and standard deviation for unanchored system is $27.05\% \pm 12.53\%$, for anchored is $33.09\% \pm 23.24\%$, and for anchored with U is $27.33\% \pm 23.29\%$.

Similarly to tensile tests, the potential influence of coating system on exploitation of the fibres was assessed for beams. Fig. 17 shows the ratio ultimate load/control load for coated and uncoated textile. The distribution is not normal and there are no statistical differences between groups. The mean and standard deviation were $26.91\% \pm 19.61\%$ for impregnated grids and $40.37\% \pm 33.23\%$ for dry ones. The failure mode of beams reinforced with coated textile is a desired one (support, tensile failure of textile, debonding with cohesive failure within the substrate of reinforcement or debonding at the matrix-to-support interface) in 45% of specimens while for uncoated meshes is in 44%.

Fig. 18 presents the increment of ultimate load with respect to a control load depending on the number of layers of the composite. The differences between groups were statistically analysed. The distribution is not normal, and it was found that some of the significant statistical difference exists between some of the groups. The ANOVA test employed was Kruskal-Wallis with a significance p-value of 0.05. The mean and standard deviation for beam with 1, 2, 3 or 4 layers was $31.77\% \pm 19.04\%$, $20.51\% \pm 23.35\%$, $42.20\% \pm 25.05\%$ and $47.11\% \pm 39.69\%$, respectively. There is no statistical difference between groups with 1, 3 and 4 layers, and between 2 and 4 layers. The differences are mainly due to the variability of the mechanical properties of the FRCM systems as well as those of the support, and not so significantly to the number of layers of textile employed.

Also, the influence of compressive strength of concrete support and of internal reinforcement in the overall behaviour of beams was analysed, as can be observed in Fig. 19 and 20. Compressive strength of the support usually ranges between 20 and 50 MPa and, even if there is not a strong correlation, generally the ratio ultimate load/control load increased with the compressive strength. It should be noted from the Fig. 20 that steel reinforcement ratio had no correlation with the increment of the ultimate load.

IV. CONCLUSIONS

In this paper, 44 research papers were systematically reviewed to study the current state of the art for tensile characterization of FRCM and for flexural reinforcement of beams.

It was concluded that the large scatter prevents generalization of parameters affecting the tensile performance of FRCM systems. Nevertheless, it was observed that trilinear behaviour in the stress-strain curves only appeared when clamping systems were employed. Also, for specimens with the same mortar and grid, clamping system obtained better results in terms of ultimate load. The cracking resistance of the FRCM was not found to affect the ultimate strength, the ratio between ultimate strength and cracking resistance is between 2 and 4 for the FRCM systems with the highest ultimate strength. The tensile strength of the mortar neither affects the relationship of ultimate and cracking strengths, as the highest ratios were found for strengths below 5 MPa.

For flexural tests, it was assessed the prevalence of the different failure modes, and it was analysed in terms of increment of load with respect to control specimens. The result for each beam was found to be a relationship between the support (concrete) strength, the reinforcement design and the test type, more than an effect of a particular parameter. However, it should be noted that a weak correlation was found between the support compressive strength and the ratio ultimate load/control load.

The constructed database allowed observing the ranges of tensile strength of FRCM and of increment of strength in reinforced concrete beams. This is a starting point for further research on configurations, following the observation of the optimal results from literature..

REFERENCES

- Akbari Hadad, H., Erickson, B., & Nanni, A. (2020). Flexural analysis and design of FRCM-strengthened RC beams. *Construction and Building Materials*, *244*, 118371. <https://doi.org/10.1016/j.conbuildmat.2020.118371>
- Akbari Hadad, H., Nanni, A., Ebead, U. A., & El Refai, A. (2018). Static and Fatigue Performance of FRCM-Strengthened Concrete Beams. *Journal of Composites for Construction*, *22*(5). [https://doi.org/10.1061/\(ASCE\)CC.1943-5614.0000868](https://doi.org/10.1061/(ASCE)CC.1943-5614.0000868)
- Arboleda, D. (2014). Fabric reinforced cementitious matrix (FRCM) composites for infrastructure strengthening and rehabilitation: Characterization methods. In *Faculty of the University of Miami* (Issue October 2013).
- Arboleda, D., Carozzi, F. G., Nanni, A., & Poggi, C. (2016). Testing Procedures for the Uniaxial Tensile Characterization of Fabric-Reinforced Cementitious Matrix Composites. *Journal of Composites for Construction*, *20*(3), 04015063. [https://doi.org/10.1061/\(ASCE\)CC.1943-5614.0000626](https://doi.org/10.1061/(ASCE)CC.1943-5614.0000626)
- Ascione, L., De Felice, G., & De Santis, S. (2015). A qualification method for externally bonded Fibre Reinforced Cementitious Matrix (FRCM) strengthening systems. *Composites Part B: Engineering*, *78*, 497–506. <https://doi.org/10.1016/j.compositesb.2015.03.079>
- Awani, O., Refai, A. El, & El-Maaddawy, T. (2015). Bond characteristics of carbon fabric-reinforced cementitious matrix in double shear tests. *Construction and Building Materials*, *101*, 39–49. <https://doi.org/10.1016/j.conbuildmat.2015.10.017>
- Bellini, A., Bovo, M., & Mazzotti, C. (2019). Experimental and numerical evaluation of fiber-matrix interface behaviour of different FRCM systems. *Composites Part B: Engineering*, *161*, 411–426. <https://doi.org/10.1016/j.compositesb.2018.12.115>
- Bertolesi, E., Carozzi, F. G., Milani, G., & Poggi, C. (2014). Numerical modeling of Fabric Reinforce Cementitious Matrix composites (FRCM) in tension. *Construction and Building Materials*, *70*, 531–548. <https://doi.org/10.1016/j.conbuildmat.2014.08.006>
- Bilotta, A., Ceroni, F., Lignola, G. P., & Prota, A. (2017). Use of DIC technique for investigating the behaviour of FRCM materials for strengthening masonry elements. *Composites Part B: Engineering*, *129*, 251–270. <https://doi.org/10.1016/j.compositesb.2017.05.075>
- Bressan, J., Ghrib, F., & El Ragaby, A. (2022). FRCM Strengthening of Corrosion-Damaged RC Beams Subjected to Monotonic and Cyclic Loading. *Journal of Composites for Construction*, *26*(1). [https://doi.org/10.1061/\(ASCE\)CC.1943-5614.0001180](https://doi.org/10.1061/(ASCE)CC.1943-5614.0001180)
- Butler, M., Mechtcherine, V., & Hempel, S. (2010). Durability of textile reinforced concrete made with AR glass fibre: Effect of the matrix composition. *Materials and Structures/Materiaux et Constructions*, *43*(10), 1351–1368. <https://doi.org/10.1617/s11527-010-9586-8>
- Caggegi, C., Carozzi, F. G., De Santis, S., Fabbrocino, F., Focacci, F., Hojdys, L., Lanoye, E., & Zuccarino, L. (2017). Experimental analysis on tensile and bond properties of PBO and aramid fabric reinforced cementitious matrix for strengthening masonry structures. *Composites Part B: Engineering*, *127*, 175–195. <https://doi.org/10.1016/j.compositesb.2017.05.048>
- Caggegi, C., Lanoye, E., Djama, K., Bassil, A., & Gabor, A. (2017). Tensile behaviour of a basalt TRM strengthening system: Influence of mortar and reinforcing textile ratios. *Composites Part B: Engineering*, *130*, 90–102. <https://doi.org/10.1016/j.compositesb.2017.07.027>
- Carozzi, F. G., Bellini, A., D'Antino, T., de Felice, G., Focacci, F., Hojdys, L., Laghi, L., Lanoye, E., Micelli, F., Panizza, M., & Poggi, C. (2017a). Experimental investigation of tensile and bond properties of Carbon-FRCM composites for strengthening masonry elements. *Composites Part B: Engineering*, *128*, 100–119. <https://doi.org/10.1016/j.compositesb.2017.06.018>
- Carozzi, F. G., Bellini, A., D'Antino, T., de Felice, G., Focacci, F., Hojdys, L., Laghi, L., Lanoye, E., Micelli, F., Panizza, M., & Poggi, C. (2017b). Experimental investigation of tensile and bond properties of Carbon-FRCM composites for strengthening masonry elements. *Composites Part B: Engineering*, *128*, 100–119.

- <https://doi.org/10.1016/j.compositesb.2017.06.018>
- Carozzi, F. G., & Poggi, C. (2015). Mechanical properties and debonding strength of Fabric Reinforced Cementitious Matrix (FRCM) systems for masonry strengthening. *Composites Part B: Engineering*, *70*, 215–230. <https://doi.org/10.1016/j.compositesb.2014.10.056>
- Choi, D., Vachirapanyakun, S., Ochirbud, M., Naidangjav, U., Ha, S., & Kim, Y. (2021). Tensile Performance, Lap-Splice Length and Behavior of Concretes Confined by Prefabricated C-FRCM System. *International Journal of Concrete Structures and Materials*, *15*(1), 45. <https://doi.org/10.1186/s40069-021-00481-w>
- Guide for the design and construction of externally bonded FRP systems for strengthening existing structures, ACI committee 440 144 (2018).
- D'Ambrisi, A., Feo, L., & Focacci, F. (2013). Experimental and analytical investigation on bond between Carbon-FRCM materials and masonry. *Composites Part B: Engineering*, *46*, 15–20. <https://doi.org/10.1016/j.compositesb.2012.10.018>
- D'Antino, T., & Papanicolaou, C. (2017). Mechanical characterization of textile reinforced inorganic-matrix composites. *Composites Part B: Engineering*, *127*, 78–91. <https://doi.org/10.1016/j.compositesb.2017.02.034>
- D'Antino, Tommaso, Carloni, C., Sneed, L. H., & Pellegrino, C. (2014). Matrix-fiber bond behavior in PBO FRCM composites: A fracture mechanics approach. *Engineering Fracture Mechanics*, *117*, 94–111. <https://doi.org/10.1016/j.engfracmech.2014.01.011>
- D'Antino, Tommaso, & Papanicolaou, C. (2017). Mechanical characterization of textile reinforced inorganic-matrix composites. *Composites Part B: Engineering*, *127*, 78–91. <https://doi.org/10.1016/j.compositesb.2017.02.034>
- D'Antino, Tommaso, & Papanicolaou, C. (Corina). (2018). Comparison between different tensile test set-ups for the mechanical characterization of inorganic-matrix composites. *Construction and Building Materials*, *171*, 140–151. <https://doi.org/10.1016/j.conbuildmat.2018.03.041>
- De Domenico, D., Maugeri, N., Longo, P., Ricciardi, G., Gulli, G., & Calabrese, L. (2022). Clevis-Grip Tensile Tests on Basalt, Carbon and Steel FRCM Systems Realized with Customized Cement-Based Matrices. *Journal of Composites Science*, *6*(9), 275. <https://doi.org/10.3390/jcs6090275>
- de Felice, G., D'Antino, T., De Santis, S., Meriggi, P., & Roscini, F. (2020). Lessons Learned on the Tensile and Bond Behavior of Fabric Reinforced Cementitious Matrix (FRCM) Composites. *Frontiers in Built Environment*, *6*. <https://doi.org/10.3389/fbuil.2020.00005>
- de Felice, G., De Santis, S., Garmendia, L., Ghiassi, B., Larrinaga, P., Lourenço, P. B., Oliveira, D. V., Paolacci, F., & Papanicolaou, C. G. (2014). Mortar-based systems for externally bonded strengthening of masonry. *Materials and Structures/Materiaux et Constructions*, *47*(12), 2021–2037. <https://doi.org/10.1617/s11527-014-0360-1>
- De Santis, S., & De Felice, G. (2015). Tensile behaviour of mortar-based composites for externally bonded reinforcement systems. *Composites Part B: Engineering*, *68*, 401–413. <https://doi.org/10.1016/j.compositesb.2014.09.011>
- De Santis, S., Hadad, H. A., De Caso y Basalo, F., de Felice, G., & Nanni, A. (2018). Acceptance Criteria for Tensile Characterization of Fabric-Reinforced Cementitious Matrix Systems for Concrete and Masonry Repair. *Journal of Composites for Construction*, *22*(6), 04018048. [https://doi.org/10.1061/\(asce\)cc.1943-5614.0000886](https://doi.org/10.1061/(asce)cc.1943-5614.0000886)
- Donnini, J., Chiappini, G., Lancioni, G., & Corinaldesi, V. (2019). Tensile behaviour of glass FRCM systems with fabrics' overlap: Experimental results and numerical modeling. *Composite Structures*, *212*(October 2018), 398–411. <https://doi.org/10.1016/j.compstruct.2019.01.053>
- Donnini, J., Corinaldesi, V., & Nanni, A. (2016). Mechanical properties of FRCM using carbon fabrics with different coating treatments. *Composites Part B: Engineering*, *88*, 220–228. <https://doi.org/10.1016/j.compositesb.2015.11.012>
- Ebead, U., & El-Sherif, H. (2019). Near surface embedded-FRCM for flexural strengthening of reinforced concrete beams. *Construction and Building Materials*, *204*, 166–176. <https://doi.org/10.1016/j.conbuildmat.2019.01.145>
- Ebead, U., Shrestha, K. C., Afzal, M. S., El Refai, A., & Nanni, A. (2017). Effectiveness of Fabric-Reinforced Cementitious Matrix in Strengthening Reinforced Concrete Beams. *Journal of Composites for Construction*, *21*(2), 04016084. [https://doi.org/10.1061/\(asce\)cc.1943-5614.0000741](https://doi.org/10.1061/(asce)cc.1943-5614.0000741)
- El-Sherif, H., Wakjira, T. G., & Ebead, U. (2020). Flexural strengthening of reinforced concrete beams using hybrid near-surface embedded/externally bonded fabric-reinforced cementitious matrix. *Construction and Building Materials*, *238*, 117748. <https://doi.org/10.1016/j.conbuildmat.2019.117748>
- Elghazy, M., El Refai, A., Ebead, U., & Nanni, A. (2017). Effect of corrosion damage on the flexural performance of RC beams strengthened with FRCM composites. *Composite Structures*, *180*, 994–1006. <https://doi.org/10.1016/j.compstruct.2017.08.069>
- Elghazy, M., El Refai, A., Ebead, U., & Nanni, A. (2018). Corrosion-Damaged RC Beams Repaired with Fabric-Reinforced Cementitious Matrix. *Journal of Composites for Construction*, *22*(5). [https://doi.org/10.1061/\(ASCE\)CC.1943-5614.0000873](https://doi.org/10.1061/(ASCE)CC.1943-5614.0000873)
- Escrig, C., Gil, L., Bernat-Maso, E., & Puigvert, F. (2015). Experimental and analytical study of reinforced concrete beams shear strengthened with different types of textile-reinforced mortar. *Construction and Building Materials*, *83*, 248–260. <https://doi.org/10.1016/j.conbuildmat.2015.03.013>
- Estevan, L., Varona, F. B., Baeza, F. J., Torres, B., & Bru, D. (2022). Textile Reinforced Mortars (TRM) tensile behavior after high temperature exposure. *Construction and Building Materials*, *328*, 127116.

- <https://doi.org/10.1016/j.conbuildmat.2022.127116>
Feng, R., Liu, Y., Zhu, J.-H., & Xing, F. (2020). Flexural behaviour of C-FRCM strengthened corroded RC continuous beams. *Composite Structures*, *245*, 112200. <https://doi.org/10.1016/j.compstruct.2020.112200>
- Hartig, J., Jesse, F., Schicktan, K., & Häußler-Combe, U. (2012). Influence of experimental setups on the apparent uniaxial tensile load-bearing capacity of Textile Reinforced Concrete specimens. *Materials and Structures/Materiaux et Constructions*, *45*(3), 433–446. <https://doi.org/10.1617/s11527-011-9775-0>
- Jabr, A., El-Ragaby, A., & Ghrib, F. (2017). Effect of the Fiber Type and Axial Stiffness of FRCM on the Flexural Strengthening of RC Beams. *Fibers*, *5*(1), 2. <https://doi.org/10.3390/fib5010002>
- Khattak, N., Mansour, M., El-Maaddawy, T., & Ismail, N. (2021). Continuous Reinforced Concrete Beams Strengthened with Fabric-Reinforced Cementitious Matrix: Experimental Investigation and Numerical Simulation. *Buildings*, *12*(1), 27. <https://doi.org/10.3390/buildings12010027>
- Kim, H.-S., Truong, G. T., Park, S.-H., & Choi, K.-K. (2018). Tensile Properties of Carbon Fiber-Textile Reinforced Mortar (TRM) Characterized by Different Anchorage Methods. *International Journal of Concrete Structures and Materials*, *12*(1), 73. <https://doi.org/10.1186/s40069-018-0296-x>
- Kim, H.-Y., You, Y.-J., & Ryu, G.-S. (2021). Reinforced Concrete Slabs Strengthened with Carbon Textile Grid and Cementitious Grout. *Materials*, *14*(17), 5046. <https://doi.org/10.3390/ma14175046>
- Kim, H.-Y., You, Y.-J., & Ryu, G.-S. (2022). Flexural Strengthening of RC Slabs with Lap-Spliced Carbon Textile Grids and Cementitious Grout. *Materials*, *15*(8), 2849. <https://doi.org/10.3390/ma15082849>
- Kim, H.-Y., You, Y.-J., Ryu, G.-S., Koh, K.-T., Ahn, G.-H., & Kang, S.-H. (2020). Flexural Strengthening of Concrete Slab-Type Elements with Textile Reinforced Concrete. *Materials*, *13*(10), 2246. <https://doi.org/10.3390/ma13102246>
- Leone, M., Aiello, M. A., Balsamo, A., Carozzi, F. G., Ceroni, F., Corradi, M., Gams, M., Garbin, E., Gattesco, N., Krajewski, P., Mazzotti, C., Oliveira, D., Papanicolaou, C., Ranocchiai, G., Roscini, F., & Saenger, D. (2017). Glass fabric reinforced cementitious matrix: Tensile properties and bond performance on masonry substrate. *Composites Part B: Engineering*, *127*, 196–214. <https://doi.org/10.1016/j.compositesb.2017.06.028>
- Lignola, G. P., Caggegi, C., Ceroni, F., De Santis, S., Krajewski, P., Lourenço, P. B., Morganti, M., Papanicolaou, C. (Corina), Pellegrino, C., Prota, A., & Zuccarino, L. (2017). Performance assessment of basalt FRCM for retrofit applications on masonry. *Composites Part B: Engineering*, *128*, 1–18. <https://doi.org/10.1016/j.compositesb.2017.05.003>
- Mandor, A., & El Refai, A. (2022). Strengthening the hogging and sagging regions in continuous beams with fiber-reinforced cementitious matrix (FRCM): Experimental and analytical investigations. *Construction and Building Materials*, *321*, 126341. <https://doi.org/10.1016/j.conbuildmat.2022.126341>
- Mazzucco, G., D'Antino, T., Pellegrino, C., & Salomoni, V. (2018). Three-dimensional finite element modeling of inorganic-matrix composite materials using a mesoscale approach. *Composites Part B: Engineering*, *143*(December 2017), 75–85. <https://doi.org/10.1016/j.compositesb.2017.12.057>
- Ombres, L. (2015). Analysis of the bond between Fabric Reinforced Cementitious Mortar (FRCM) strengthening systems and concrete. *Composites Part B: Engineering*, *69*, 418–426. <https://doi.org/10.1016/j.compositesb.2014.10.027>
- Ombres, L., Mancuso, N., Mazzuca, S., & Verre, S. (2019). Bond between Carbon Fabric-Reinforced Cementitious Matrix and Masonry Substrate. *Journal of Materials in Civil Engineering*, *31*(1), 04018356. [https://doi.org/10.1061/\(ASCE\)MT.1943-5533.0002561](https://doi.org/10.1061/(ASCE)MT.1943-5533.0002561)
- Papanicolaou, C. G., & Papanitiou, I. C. (2016). Optimum design of textile-reinforced concrete as integrated formwork in slabs. In *Textile Fibre Composites in Civil Engineering* (pp. 246–274).
- Papanicolaou, Catherine G., Triantafyllou, T. C., Papanitiou, M., & Karlos, K. (2008). Textile reinforced mortar (TRM) versus FRP as strengthening material of URM walls: Out-of-plane cyclic loading. *Materials and Structures/Materiaux et Constructions*, *41*(1), 143–157. <https://doi.org/10.1617/s11527-007-9226-0>
- Peled, A., & Bentur, A. (2000). Geometrical characteristics and efficiency of textile fabrics for reinforcing cement composites. *Cement and Concrete Research*, *30*(5), 781–790. [https://doi.org/10.1016/S0008-8846\(00\)00239-8](https://doi.org/10.1016/S0008-8846(00)00239-8)
- Peled, A., Cohen, Z., Pasher, Y., Roye, A., & Gries, T. (2008). Influences of textile characteristics on the tensile properties of warp knitted cement based composites. *Cement and Concrete Composites*, *30*(3), 174–183. <https://doi.org/10.1016/j.cemconcomp.2007.09.001>
- Peled, A., Mobasher, B., & Bentur, A. (2017). Textile reinforced concrete. In *Textile Reinforced Concrete* (1st editio). CRC Press. <https://doi.org/10.1201/9781315119151>
- Raoof, S. M., & Bournas, D. A. (2017). TRM versus FRP in flexural strengthening of RC beams: Behaviour at high temperatures. *Construction and Building Materials*, *154*, 424–437. <https://doi.org/10.1016/j.conbuildmat.2017.07.195>
- Raoof, S. M., Koutas, L. N., & Bournas, D. A. (2017). Textile-reinforced mortar (TRM) versus fibre-reinforced polymers (FRP) in flexural strengthening of RC beams. *Construction and Building Materials*, *151*, 279–291. <https://doi.org/10.1016/j.conbuildmat.2017.05.023>
- Rodríguez-Marcos, M., Villanueva-Llaurado, P., Fernández-Gómez, J., & López-Rebollo, J. (2023). Improvement of tensile properties of carbon fibre-reinforced cementitious matrix composites with coated textile and enhanced mortars. *Construction and Building Materials*,

- 369(February), 130552. <https://doi.org/10.1016/j.conbuildmat.2023.130552>
- Su, Mei-ni, Wei, L., Zeng, Z., Ueda, T., Xing, F., & Zhu, J.-H. (2019). A solution for sea-sand reinforced concrete beams. *Construction and Building Materials*, 204, 586–596. <https://doi.org/10.1016/j.conbuildmat.2019.01.146>
- Su, Mei-ni, Wei, L., Zhu, J.-H., Ueda, T., Guo, G., & Xing, F. (2019). Combined Impressed Current Cathodic Protection and FRCM Strengthening for Corrosion-Prone Concrete Structures. *Journal of Composites for Construction*, 23(4). [https://doi.org/10.1061/\(ASCE\)CC.1943-5614.0000949](https://doi.org/10.1061/(ASCE)CC.1943-5614.0000949)
- Su, Mei-ni, Zeng, C., Li, W., Zhu, J.-H., Lin, W., Ueda, T., & Xing, F. (2020). Flexural performance of corroded continuous RC beams rehabilitated by ICCP-SS. *Composite Structures*, 232, 111556. <https://doi.org/10.1016/j.compstruct.2019.111556>
- Su, Mei ni, Wang, Z., & Ueda, T. (2022). Optimization and design of carbon fabric-reinforced cementitious matrix composites. *Structural Concrete*, 23(3), 1845–1860. <https://doi.org/10.1002/suco.202000801>
- Tekieli, M., De Santis, S., de Felice, G., Kwiecień, A., & Roscini, F. (2017). Application of Digital Image Correlation to composite reinforcements testing. *Composite Structures*, 160, 670–688. <https://doi.org/10.1016/j.compstruct.2016.10.096>
- Tetta, Z. C., & Bournas, D. A. (2016). TRM vs FRP jacketing in shear strengthening of concrete members subjected to high temperatures. *Composites Part B: Engineering*, 106, 190–205. <https://doi.org/10.1016/j.compositesb.2016.09.026>
- Tran, H. Van, Truong, G. T., & Choi, K.-K. (2019). Effect of Harsh Conditions on the Tensile Behaviour of Lap-Spliced Carbon Fiber Textile-Reinforced Mortar (TRM) with Different Surface Treatment Methods. *Applied Sciences*, 9(15), 3087. <https://doi.org/10.3390/app9153087>
- Truong, V. D., Lee, D. H., & Kim, D. J. (2021). Effects of different grips and surface treatments of textile on measured direct tensile response of textile reinforced cementitious composites. *Composite Structures*, 278, 114689. <https://doi.org/10.1016/j.compstruct.2021.114689>
- Valluzzi, M. R., Modena, C., & de Felice, G. (2014). Current practice and open issues in strengthening historical buildings with composites. *Materials and Structures/Materiaux et Constructions*, 47(12), 1971–1985. <https://doi.org/10.1617/s11527-014-0359-7>
- Wei, L. L., Zhu, J. H., Ueda, T., Su, M. N., Liu, J., Liu, W., Tang, L. P., & Xing, F. (2020). Tensile behaviour of carbon fabric reinforced cementitious matrix composites as both strengthening and anode materials. *Composite Structures*, 234. <https://doi.org/10.1016/j.compstruct.2019.111675>
- Wei, L., Ueda, T., Matsumoto, K., & Zhu, J.-H. (2021). Experimental and analytical study on the behavior of RC beams with externally bonded carbon-FRCM composites. *Composite Structures*, 273, 114291. <https://doi.org/10.1016/j.compstruct.2021.114291>
- Younis, A., Ebead, U., & Shrestha, K. (2020). Tensile characterization of multi-ply fabric-reinforced cementitious matrix strengthening systems. *Structural Concrete*, 21(2), 713–723. <https://doi.org/10.1002/suco.201900076>



Reconocimiento – NoComercial (by-nc): Se permite la generación de obras derivadas siempre que no se haga un uso comercial. Tampoco se puede utilizar la obra original con finalidades comerciales.